

Supporting Information

Machine learning methodology to investigate the lattice thermal conductivity of defected PbTe

Mi Qin^{a, b}, Xuemei Zhang^{c, d}, Jianbo Zhu^e, Yuming Yang^a, Zhuoyang Ti^a, Yaoling Shen^a, Xianlong Wang^a, Xiaobing Liu^{* f}, and Yongsheng Zhang^{* f}

^aKey Laboratory of Materials Physics, Institute of Solid State Physics, HFIPS, Chinese Academy of Sciences, Hefei 230031, China

^bScience Island Branch of Graduate School, University of Science and Technology of China, Hefei 230026, China

^cSchool of Physics and Electronic Information Engineering, Ningxia Normal University, Guyuan, 756000, China

^dEngineering Technology Research Centre for Nano-structures and Functional Materials, Ningxia Normal University, Guyuan, 756000, China

^eState Key Laboratory of Advanced Welding and Joining, Harbin Institute of Technology, Harbin 150001, China.

^fAdvanced Research Institute of Multidisciplinary Sciences, Qufu Normal University, Qufu, Shandong Province, 273165, China

* Corresponding author

Email: xiaobing.phy@qfnu.edu.cn

yshzhang@qfnu.edu.cn

Non-equilibrium molecular dynamics for lattice thermal conductivity calculations

In a non-equilibrium molecular dynamics (NEMD) simulation for the thermal conductivity calculations, a heat flux is imposed through the box by adding heat to atoms inside a hot source (heat source) in one interval of the box and extracting the identical rate of heat from atoms inside a cold source (heat sink) in another coordinate of the box. After reaching equilibrated state in the atomic system, the thermal conductivity of the atoms in the box was calculated via Fourier's law¹:

$$\kappa_l = \frac{Q}{dT/dz}$$

where Q is the heat flux, z is the direction of heat flow and dT/dz is the temperature gradient in the z -direction.

NEMD can be performed using our trained NNP potentials. The cross-section size of simulation cell is about $48.27 \times 46.45 \text{ \AA}^2$. The periodic boundary conditions are imposed in all three directions. The NVT ensemble is first used to equilibrate the system at zero pressure for 200 ps with a time step of 2.0 fs. Subsequently, atomic positions within the outmost layer at the end of the simulation domain are fixed, and 5 nm region atoms next to the fixed part are thermostatted using the Langevin dynamics to create and maintain a temperature gradient across the system. A temperature difference of 60 K is applied across the system through the thermostatted regions. The cold ($T_{cold} = 270$ K) and hot ($T_{hot} = 330$ K) Nosé-Hoover reservoirs are applied on the right end and the left end of the simulation domain, respectively. Then, the system is simulated in a NVE for 4 ns to obtain a steady temperature gradient and stable heat current. In the next 3 ns of simulation time, the temperature data are collected at a time interval of 200 ps and averaged to get the final temperature gradient for minimization of statistical fluctuations. Then, by applying the temperature gradient, the heat flux reaches the steady-state after 4 ns, fluctuating around the steady-state value. The accumulative energies added into the hot regions or removed from the cold regions were saved to calculate the heat flux.

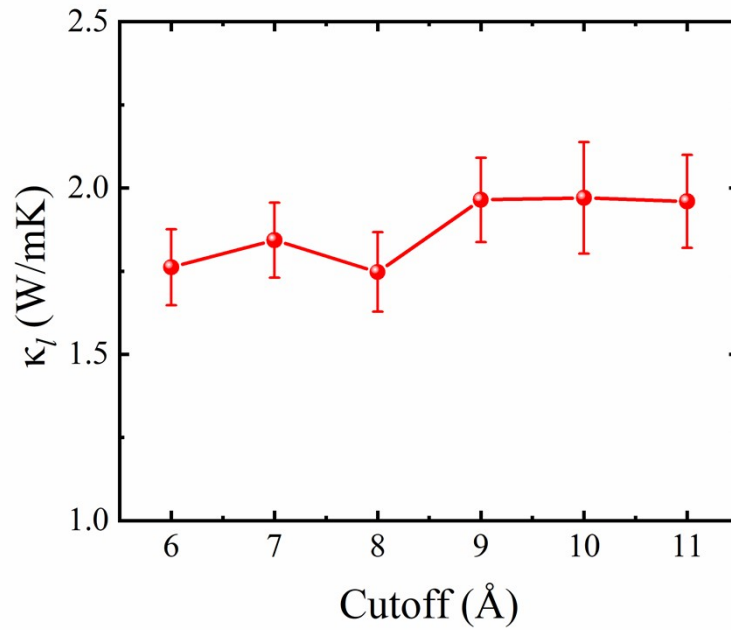


Figure S1. The calculated thermal conductivities of bulk PbTe at 300 K versus cutoff radius in the training processes.

Different cutoff radii are used in the training process to produce the NNP potentials. These potentials are then used to test the convergency of the lattice thermal conductivity of PbTe at 300 K (Fig. S1). We can find that the lattice thermal conductivity of PbTe is converged to within 0.01 W/mK at the cutoff radius of 9.0 Å. Thus, the cutoff radius of 9 Å is the optimal value to describe the range interactions in PbTe.

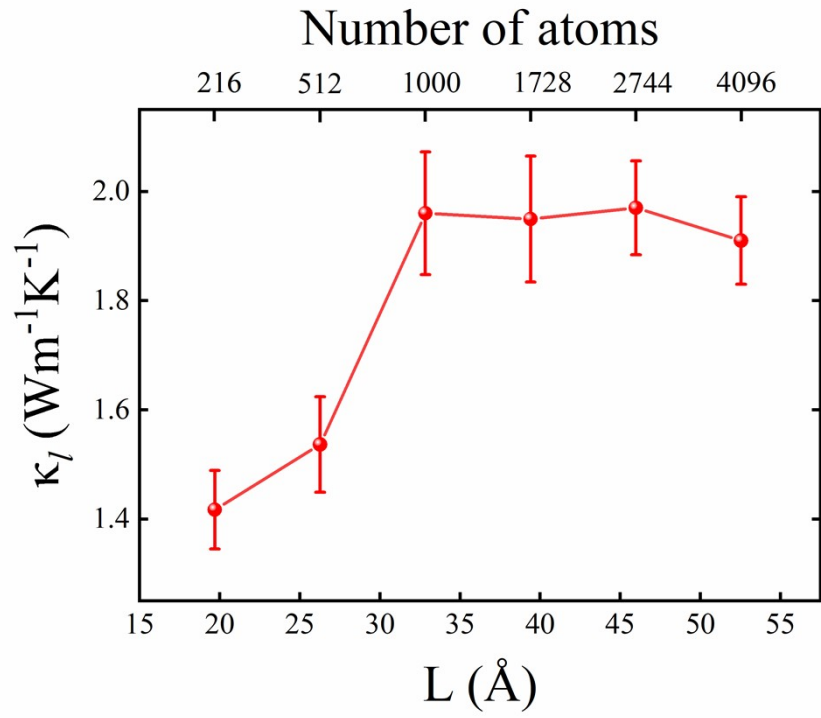


Figure S2. Thermal conductivity (κ) of PbTe at 300 K as a function of the linear size (L) of the cubic simulation cell and the number of PbTe atoms. A $5 \times 5 \times 5$ ($a = 32.8 \text{ \AA}$, containing 1000 atoms) supercell can converge the lattice thermal conductivity.

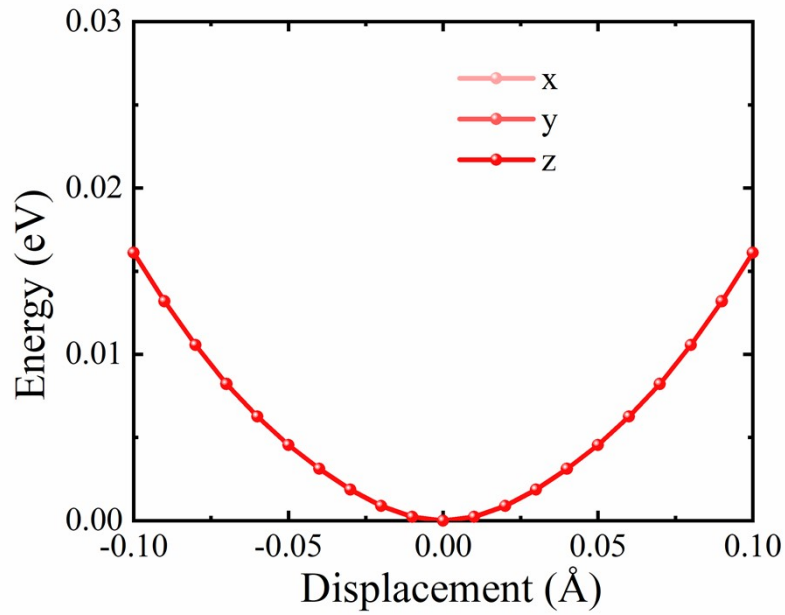


Figure S3. The calculated potential energy surface as a function of atomic displacement around the equilibrium positions along the x, y, and z directions for the bulk PbTe.

We focus on the lattice thermal conductivity of bulk PbTe, not those with significantly structure distortion or liquid. In the bulk PbTe, the bond length of Pb-Te is 3.28 Å. Thus, the largest displacement 0.04 Å is only ~1% of the bond length, which can be treated as a small perturbation to the bond. It would not change the Pb-Te bond or the crystal structure a lot. On the other hand, from the potential energy surface plot of PbTe (Fig. S3), we notice that the 0.04 Å displacement from its equilibrium position is still within the harmonic parabolic region. Thus, 0.04 Å is a reasonable value to shift atom and still keep the structure without the significant distortion.

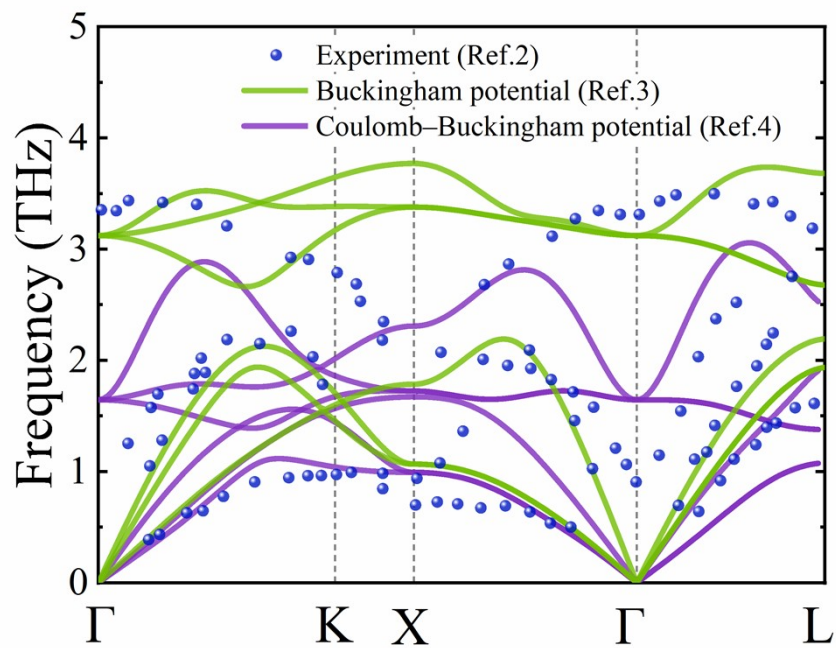


Figure S4. Phonon dispersions from experimental measurements² (the blue dots) and calculated using the empirical potentials (the Buckingham potential³: the solid green lines, and the Coulomb-Buckingham potential⁴: the solid purple lines).

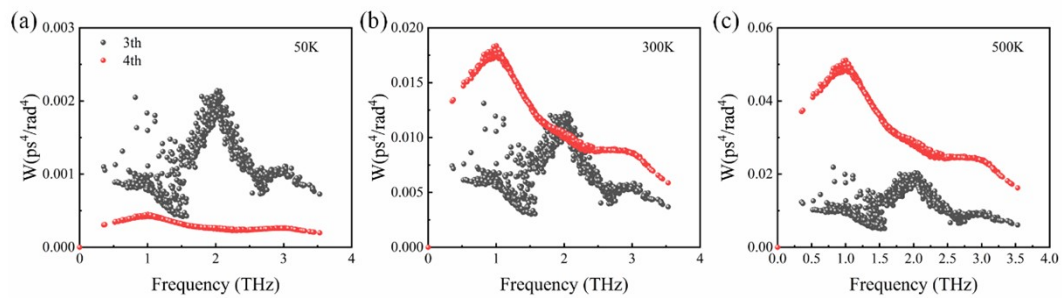


Figure S5. The calculated weighted phase space using the three- (black dots) and four-phonon (red dots) scatterings at (a) 50, (b) 300 and (c) 500 K, respectively.

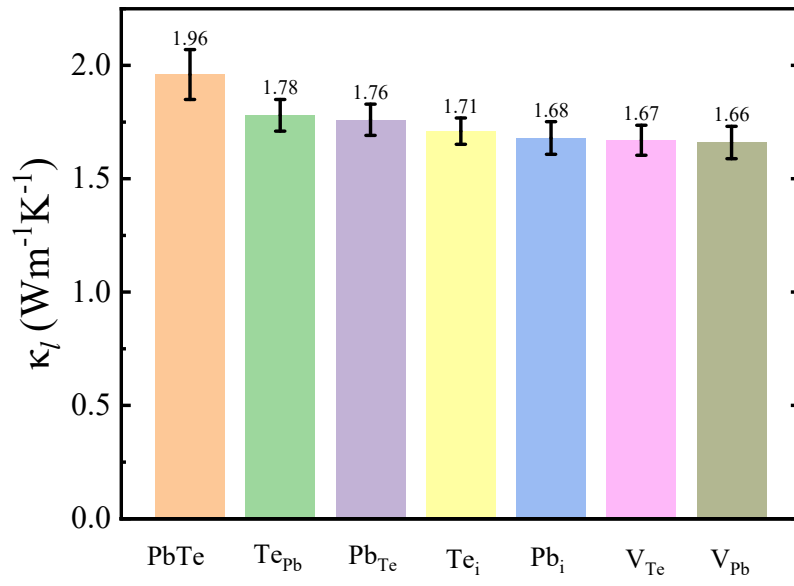


Figure S6. The lattice thermal conductivities of PbTe with different point defects (Pb_{Te} , Te_{Pb} , Pb_i , Te_i , V_{Pb} and V_{Te}) at 300K.

Table S1. The number of configurations for different systems.

System	Type	Training	Testing
Bulk	Perfect	7918	300
	Pb _i	1070	50
	Te _i	1077	50
	Pb _{Te}	976	50
	Te _{Pb}	965	50
	V _{Pb}	1065	50
	V _{Te}	1081	50
Te occupied twin boundary (Te-TB)	Perfect	1400	300
	Pb _i	1059	50
	Te _i	1100	50
	Pb _{Te}	1100	50
	Te _{Pb}	800	50
	V _{Pb}	1000	50
	V _{Te}	1100	50
Pb occupied twin boundary (Pb-TB)	Perfect	1400	300
	Pb _i	902	50
	Te _i	800	50
	Pb _{Te}	952	50
	Te _{Pb}	1000	50
	V _{Pb}	1100	50
V _{Te}	1100	50	

References

1. F. Müller-Plathe, *The Journal of Chemical Physics*, 1997, **106**, 6082-6085.
2. W. Cochran, R. A. Cowley, G. Dolling and M. M. Elcombe, *Proc. Math. Phys. Eng. Sci.*, 1997, **293**, 433-451.
3. B. Qiu, H. Bao, X. Ruan, G. Zhang and Y. Wu, 2012.
4. J. F. Troncoso, P. Aguado-Puente and J. Kohanoff, *J Phys Condens Matter*, 2020, **32**, 045701.